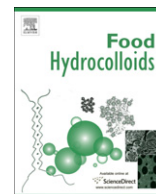




Contents lists available at ScienceDirect

## Food Hydrocolloids

journal homepage: [www.elsevier.com/locate/foodhyd](http://www.elsevier.com/locate/foodhyd)

## Co-adsorption of $\beta$ -casein and calcium phosphate nanoclusters (CPN) at hydrophilic and hydrophobic solid–solution interfaces studied by neutron reflectometry

David Follows<sup>a</sup>, Carl Holt<sup>b</sup>, Robert K. Thomas<sup>a</sup>, Fredrik Tiberg<sup>c,d</sup>, Giovanna Fragneto<sup>e</sup>, Tommy Nylander<sup>d,\*</sup>

<sup>a</sup> Physical and Theoretical Chemistry Laboratory, University of Oxford, Parks Road, Oxford OX1 3PJ, UK

<sup>b</sup> University of Glasgow, Department of Biochemistry and Cell Biology, Glasgow G12 8QQ, Scotland, UK

<sup>c</sup> Camurus AB, Ideon Science Park, Gamma Building, Sölvegatan 41, SE-223 70 Lund, Sweden

<sup>d</sup> Physical Chemistry, Department of Chemistry, Lund University, Box 124, SE-221 00 Lund, Sweden

<sup>e</sup> Institut Laue-Langevin, BP 156, 38042 Grenoble, France

## ARTICLE INFO

## Article history:

Received 24 April 2010

Accepted 1 September 2010

## Keywords:

 $\beta$ -casein

Calcium phosphate nanoclusters

Adsorption

Neutron reflectometry

## ABSTRACT

Neutron reflectometry was used to study the co-adsorption of calcium phosphate nanoclusters (CPN) and  $\beta$ -casein at hydrophobized and hydrophilic silica–water interfaces. The structural characteristics of the adsorbed layer were determined from neutron reflectivity curves analysed with multi-layer optical models. We used a highly specific proteolytic enzyme, endoproteinase Asp-N in conjunction with a single neutron contrast to verify the model of the protein layer structure. The results showed that the calcium phosphate nanoclusters profoundly affected the rate of adsorption and structure of the interface compared to the adsorption of  $\beta$ -casein alone and for the hydrophobic interface the effects depended on the point at which the nanoclusters were added. It is proposed that the nanoclusters become surface active because whole  $\beta$ -casein molecules can replace one or more of the hydrophilic peptides in the shell of the nanoclusters.

© 2010 Published by Elsevier Ltd.

## 1. Introduction

$\beta$ -casein (together with  $\alpha_{S1}$ -casein) is the most abundant protein among the four caseins present in cow's milk (Dickinson, 1999). Above 4 °C it readily forms surfactant micelle-like aggregates in aqueous solution starting at a concentration 0.5 mg/ml (Leclerc & Calmettes, 1997; Payens & Vreeman, 1982). The biological role of casein molecules includes the sequestration of amorphous calcium phosphate to form stable complexes in milk (Holt, 1998; C. Holt & Sawyer, 1988; Holt, Wahlgren, & Drakenberg, 1996; Walstra & Jenness, 1984). Caseins are also frequently used as additives in food, paint, glue and coating colours for paper (Walstra & Jenness, 1984). Knowledge of the mechanisms by which caseins adsorb is therefore of great interest in many colloid-related industries.

The average hydrophobicity of the amino acid residues in  $\beta$ -casein is less than that of a typical globular protein and more than that of a typical natively unfolded protein. The N-terminal 21 residues contain most of the charged residues and sites of phosphorylation whereas the remainder is mostly uncharged and

contains a few short hydrophobic sequences. To a degree, this gives the protein an amphiphilic character with a hydrophilic N-terminal head and a so-called “hydrophobic” tail, though it is only relatively hydrophobic compared to the head.

Studies of  $\beta$ -casein adsorption have mainly been performed at hydrophobic surfaces by a number of experimental techniques such as ellipsometry, surface force measurements, dynamic light scattering, neutron reflectivity, and wetting force measurements (Atkinson, Dickinson, Horne, & Richardson, 1995; Brooksbank, Davidson, Horne, & Leaver, 1993; Dagleish & Leaver, 1991; Dickinson, Horne, Phipps, & Richardson, 1993; Fragneto, Thomas, Rennie, & Penfold, 1995; Kull, Nylander, Tiberg, & Wahlgren, 1997; Leaver & Dagleish, 1992; Mackie, Mingins, & North, 1991; Nylander & Tiberg, 1999; Nylander & Wahlgren, 1994, 1997). The common model emerging from these studies is that the protein forms a monolayer at hydrophobic surfaces, with the “hydrophobic” part of the protein sticking to the surface and the highly charged N-terminal portion protruding into the solution. The main driving force for adsorption at hydrophobic surfaces is entropic due to the de-solvation of adsorbed sequences. This model of adsorption at hydrophobic surfaces was also experimentally verified by sensibly studying the effects of a specific proteolytic enzyme (endoproteinase Asp-N) on the interfacial  $\beta$ -casein

\* Corresponding author. Tel.: +46 462228158; fax: +46 462224413.

E-mail address: [Tommy.Nylander@fkem1.lu.se](mailto:Tommy.Nylander@fkem1.lu.se) (T. Nylander).

layer (Kull et al., 1997; Nylander & Wahlgren, 1994). Endoproteinase Asp-N can potentially cleave the  $\beta$ -casein molecule at four different sites where two are located close to the hydrophilic region (residues 43 and 47) and two in the “hydrophobic” region (residues 129 and 184) (Drapeau, 1980; Wahlgren, 1992). The results obtained at hydrophobic surfaces indicated that the enzyme could cleave the sites in the hydrophilic part of the protein and the rest of the adsorbed protein layer seemed to remain intact. This confirms that the protein adopts a brush-like structure when adsorbed onto hydrophobic surfaces with its hydrophilic sequence exposed to the solution.

Numerous studies indicate that the caseins interact with amorphous calcium phosphate primarily through short sequences containing three or more phosphorylated residues known as casein phosphate centres (Holt, Davies, & Law, 1986; Holt et al., 1989; Ono, Ohtawa, & Takagi, 1994). Indeed, short, phosphate centre-containing peptides can sequester amorphous calcium phosphate to form core-shell nanoparticles with the core comprising the calcium phosphate and the shell composed of 50 or so peptides (Holt, Timmins, Errington, & Leaver, 1998; Holt et al., 1996; Little & Holt, 2004). The particles are called calcium phosphate nanoclusters (CPN) and the best characterised of these is the one formed by the N-terminal tryptic peptide of  $\beta$ -casein, residues 1–25. This nanocluster is used here. Calcium phosphate nanoclusters are also formed or predicted to form by a number of recombinant phosphopeptides, osteopontin phosphopeptides and at least 11 other non-casein proteins (Clegg & Holt, 2009; Holt, Sørensen, & Clegg, 2009).

In spite of the importance of  $\beta$ -casein as a stabiliser of dispersions of amorphous calcium phosphate in milk and hydrophilic colloids in general, relatively few studies of the adsorbed layer properties at hydrophilic surfaces have been conducted.

Like ellipsometry, neutron reflection also allows the measurement of the refractive index profile at an interface, but in the form of the scattering length density (Holt, 1998; Lu & Thomas, 2000; Nylander et al., 2008; Penfold et al., 1997). The main benefit here is from the difference of scattering lengths between hydrogen and deuterium, which allows for contrast variation/optimisation by substituting  $\text{H}_2\text{O}$  with  $\text{D}_2\text{O}$ . Hence, the sensitivity of neutron reflection to the layer structure depends on the scattering length density of the components of the layer and the surrounding bulk media. The possibility of measuring at different contrasts allows for the application of more suitable multilayer models to interpret the adsorption data with a good degree of confidence. The inhomogeneity of the protein layer in the normal direction can be revealed by applying such models. Here we also show that one can use a highly specific proteolytic enzyme in conjunction with a single neutron contrast to explore the structure of a protein layer in more detail than with conventional contrast variation alone (Nylander, Tiberg, Su, Lu, & Thomas, 2001).

## 2. Materials and methods

The  $\beta$ -casein (genetic variant A<sup>1</sup>,  $M_w = 24000$  g/mole) was extracted from bovine milk and purified according to the procedure described by Nylander and Wahlgren (Nylander & Wahlgren, 1994). Endoproteinase Asp-N was purchased from Boehringer Mannheim Biochemica (now Roche Diagnostics) (Cat. 1054589, Lot 14184025). The water used was purified by a Milli-Q system from Millipore Corporation, Bedford, MA giving water with resistivity of 18 M $\Omega$ cm and low bubble persistence. Deuterated water (99.9%, deuterated) was obtained from Fluorochem. All other chemicals used were of analytical grade.  $\beta$ -Casein (0.1 mg/ml) or endoproteinase Asp-N (0.04  $\mu$ g/ml) were dissolved in 50 ml 0.02 M imidazole-HCl buffer (pH 7.0) containing 17 mM  $\text{CaCl}_2$ . All aqueous  $\text{H}_2\text{O}$  and  $\text{D}_2\text{O}$  solutions featured in this study were buffered similarly. Fresh solutions were always prepared immediately before the adsorption measurement

was started. The calcium phosphate nanoclusters were prepared with  $\beta$ -casein 4P (f1-25) at a concentration of 5 mg/ml in either  $\text{H}_2\text{O}$  or  $\text{D}_2\text{O}$  by the method of Holt et al. (Holt et al., 1998). They are spherical in shape with an average core radius of 24 Å and a shell outer radius of 40 Å. Calculation of the equilibria in the nanocluster solution showed that 90% of the peptide was sequestering the calcium phosphate at pH 6.7 and 100% at pH 7.0 (Little & Holt, 2004). Samples were diluted to the required concentration and the adsorption surface washed with a calcium and phosphate-containing dilution buffer saturated in calcium phosphate so that the nanoclusters did not dissociate. This is important as dilution with water or calcium free buffer can destabilise the system.

The neutron reflection measurements were made on the ‘white beam’ time of flight reflectometer D17 at the Institut Laue-Langevin, Grenoble, France (Cubitt & Fragneto, 2002). Neutron wavelengths from 2.2 to 19 Å were used in these experiments. The sample cell consisted of a Teflon trough clamped against a silicon block of dimensions 12.50  $\times$  5.08  $\times$  2.54 cm (Fragneto, Lu, McDermott, & Thomas, 1996). The collimated beam enters the end of the silicon block at a fixed angle, is then reflected at a glancing angle from the solid-liquid interface, and exits from the opposite end of the silicon block. Each reflectivity profile was measured at two different glancing angles of 0.8° and 4°, respectively. The intensity of the reflected beam over the intensity of the incoming beam (reflectivity) as a function of the momentum (wave vector) transfer  $Q = 4\pi/\lambda (\sin \theta)$ , where  $\lambda$  is the wavelength and  $\theta$  is the glancing angle of incidence, was determined and the results for the two angles were then combined. The background recorded simultaneously with the reflectivity measurements by the 2-dimensional <sup>3</sup>He gas detector to the side of the specular ridge was subtracted from the recorded data. The background for the  $\text{D}_2\text{O}$  runs was typically  $2 \times 10^{-6}$  given in terms of reflectivity (see next section).

The procedure for polishing the large face (111) of the silicon blocks has been described earlier (Fragneto et al., 1996). The large face was polished using an Engis polishing machine, on a mat using a 1-micron silica suspension followed by colloidal alumina. The blocks were then cleaned in a three-step process. They were first rinsed in water purified by a Milli-Q system from Millipore Corporation, Bedford, MA (water resistivity of 18 M $\Omega$ cm<sup>-1</sup>). Then, they were soaked in a solution consisting of water, sulphuric acid (98%) and hydrogen (27.5% peroxide solution in water) mixed in a volume ratio of 5:4:1 respectively at 80 °C for 40 min. The blocks were then removed from the cleaning solution and allowed to cool for a few minutes before being quenched by immersion in Milli-Q water. Finally, they were placed in a stream of oxygen and exposed to ultraviolet light for 30 min. This procedure rendered the surfaces hydrophilic and highly reproducible with respect both to the silicon oxide layer thickness and the  $\beta$ -casein adsorption. Before the adsorption measurements were started, the oxide layer at the surface of the silicon block was characterised in terms of structural parameters. The characterisation was done in different isotopic compositions of water in order to reveal features of the bare substrate such as roughness and oxide layer thickness. The water contrasts used were pure  $\text{D}_2\text{O}$  (scattering length density of  $6.35 \times 10^{-6}$  Å<sup>-2</sup>), water CMSi ( $\text{H}_2\text{O}/\text{D}_2\text{O}$  weight ratio of 0.595/0.405 and scattering length density of  $2.07 \times 10^{-6}$  Å<sup>-2</sup>), and finally pure  $\text{H}_2\text{O}$  (scattering length density of  $-0.56 \times 10^{-6}$  Å<sup>-2</sup>). Two batches of silicon blocks were used. The combined fitting gave an oxide layer thickness of  $14 \pm 2$  Å for the batch used for silanisation  $9 \pm 1$  Å for the other. The scattering length density for both blocks was  $3.4 \times 10^{-6}$  Å<sup>-2</sup>. This scattering length density is the same value as that expected for amorphous silica, suggesting little penetration of water into the layer and hence a surface free of defects. The surface roughness was calculated to be  $\leq 2-3$  Å as the fit of the model could not be improved by using roughness values of 0 or 2–3 Å.

The hydrophobic surface was then prepared on some of the silicon blocks by immersing them in a stirred 2 mM solution of perdeuterated octadecyltrichlorosilane (d-OTS) in hexadecane in a Teflon beaker overnight at 20°C (Fragneto et al., 1995). The coated blocks were then washed with dichloromethane, then ethanol and finally pure H<sub>2</sub>O. This procedure gave a chemisorbed layer of d-OTS free from defects with a thickness of  $29 \pm 2$  Å. The scattering length density of the block used for the simultaneous addition of CPN and  $\beta$ -casein was  $6.0 \times 10^{-6}$  Å<sup>-2</sup> while the block used for the sequential adsorption studies had a somewhat higher value of  $6.7 \times 10^{-6}$  Å<sup>-2</sup>, suggesting a somewhat higher density of deuterated material in the self-assembled d-OTS layer, but both surfaces were considered to be very hydrophobic with a water contact angle >90°. The surface roughness was again calculated to be  $\leq 2-3$  Å as the fit of the model could not be improved by using roughness values of 0 or 2–3 Å.

### 2.1. Data evaluation

In a typical neutron reflection (NR) experiment, both incoming and reflected beam intensities are monitored and the ratio of the two is the reflectivity, *R*. The neutron reflectivity is determined as a function of momentum transfer, *Q*, and the obtained reflectivity profile is determined by the variation of the scattering length density,  $\rho$ , along the normal to the surface. In turn the scattering length density depends on the chemical composition of the sample as (cf. (Efimova, van Well, Hanefeld, Wierczinski, & Bouwman, 2005; Holt, 1998)) and is given by:

$$\rho = \sum n_i b_i \quad (1)$$

where  $n_i$  is the number density of element *i* and  $b_i$  its scattering amplitude (scattering length). In comparison with techniques such as ellipsometry and X-ray reflection, the main advantage of neutron reflection is that the scattering length or scattering amplitude varies from isotope to isotope, not just element to element. Exploiting isotopic substitution can thus generate different reflectivity profiles. This feature has proved very effective in revealing the structure of complicated interfaces.

The derivation of structural information from reflectivity profiles is usually done by means of the optical matrix formalism which has been described in detail elsewhere (Born & Wolf, 1980). A typical modelling procedure usually starts with an assumption of a structural model for the adsorbed layer, followed by calculation of the reflectivity based on the optical matrix formula. The calculated reflectivity is then compared with the measured data and the structural parameters are then varied by least-squares iteration until a best fit is found. The structural parameters used in the fitting are the number of layers, thickness (*d*), and the corresponding scattering length density ( $\rho$ ) for each layer.

The area per molecule, *A*, can be deduced directly from the derived scattering length density and thickness of the layer using

$$A = \frac{\sum m_i b_i + n_w b_w}{\rho d} \quad (2)$$

where, in our case,  $\sum m_i b_i$  denotes the total scattering length of the protein molecule,  $n_w$  is the number of water molecules associated with each protein molecule and  $b_w$  is the scattering length of water. The value of  $n_w$  can be estimated from the following equation

$$n_w = \frac{Ad - V_p}{V_w} \quad (3)$$

where  $V_p$  and  $V_w$  are the molecular volumes for protein and water respectively. The volume fraction of protein,  $\phi_p$ , can be obtained from:

$$\rho = \phi_p \rho_p + (1 - \phi_p) \rho_w \quad (4)$$

where  $\rho_p$  and  $\rho_w$  are the scattering length densities of protein and water, respectively.

From *A* (or  $\phi_p$ ) the surface excess,  $\Gamma$ , can be obtained as

$$\Gamma = \frac{1}{N_a A} = \frac{d\phi_p}{(N_a V_p)/M_{wp}} = \frac{d\phi_p}{v_p} \quad (5)$$

where  $N_a$  is Avogadro's number,  $M_{wp}$  is protein molecular weight and  $v_p$  is the partial specific volume of the protein. It is important to bear in mind that the scattering length of a protein is affected by deuterium exchange in D<sub>2</sub>O. Based on a molecular volume of  $\beta$ -casein of 29594 Å<sup>3</sup> (Fragneto et al., 1995), which corresponds to a partial specific volume,  $v_p$ , of 0.7426 ml/g using the  $M_{wp}$  of  $\beta$ -casein of 24000 g/mole, the  $\rho_p$  is  $1.78 \cdot 10^{-6}$  Å<sup>-2</sup> in H<sub>2</sub>O and is  $2.76 \cdot 10^{-6}$  Å<sup>-2</sup> in D<sub>2</sub>O (Efimova et al., 2005). The overall match-point of the calcium phosphate nanoclusters occurs at 46.7% D<sub>2</sub>O (Holt et al., 1998), which corresponds to a scattering length density of  $2.67 \cdot 10^{-6}$  Å<sup>-2</sup>. In the present study we did measurements at only one contrast, 100% D<sub>2</sub>O. The basis for using D<sub>2</sub>O is that it brings the destructive part of the first fringe within the range of the experiment. In D<sub>2</sub>O the experiment has a higher resolution than it would in H<sub>2</sub>O, even though the contrast between protein layer and D<sub>2</sub>O is similar in magnitude to that between protein and H<sub>2</sub>O. Since the scattering length density of  $\beta$ -casein in the D<sub>2</sub>O contrast is similar to the CPN we used the value for the protein, which is  $2.76 \cdot 10^{-6}$  Å<sup>-2</sup>, to calculate the total volume fraction of matter in the mixed  $\beta$ -casein – nanocluster system.

Although equations (2–5) have been developed under the condition of uniform layer distribution, they are directly applicable to each of the sub-layers when more than one layer is required to model the density distribution profiles. The total adsorbed amounts are obtained by summing over the sub-layers used in the fitting procedure. The choice of the number of sub-layers is dependent upon the extent of inhomogeneity across the interfacial region. We identify the simplest model able to fit the experimental data by which we mean a model with the minimum number of sub-layers and the minimum number of fitted parameters. Simple two- or, at most, three-layer models without roughness were found to fit the data within the limits of experimental error. Three-layer models were not postulated if two layers proved adequate. An important aspect here is that the model should be physically reasonable, considering the molecular dimension of the system investigated.

The use of multiple contrasts is always an advantage in developing multilayer models. Measurement of more than one reflectivity profile, for the same interfacial system, substantially improves the reliability of the derived structural information. Most relevant to this work is the substitution of hydrogen by deuterium. However, recombinant methods are required to replace all hydrogen atoms in proteins. For biological systems this may not always be feasible due to the lack of material, time consuming sample preparation and the stability of the sample. Isotopic contrast variation can be achieved by varying the ratio of H<sub>2</sub>O to D<sub>2</sub>O.

In this work we use what we can call “chemical contrast variation”, which we previously introduced to obtain additional information regarding the layer structure from ellipsometry (Kull et al., 1997; Nylander & Wahlgren, 1994) and neutron reflectometry data (Nylander et al., 2001). If we consider a protein of known chemical structure AB, the use of a highly specific enzyme can break the AB link and only that link. In the  $\beta$ -casein case, A could represent the hydrophilic part and B the hydrophobic part. The protein then adsorbs on a surface to give a layer and the resolution of the neutron experiment is only able to see the layer as a single uniform layer. We then examine how the neutron reflectivity of the layer changes

when we break the link. Let us suppose that the molecular weights of A and B are about the same. If, after addition of the enzyme the thickness of the layer drops by half, then we can conclude that the link is accessible to the enzyme and the AB axis is normal to the surface and that we have removed either A or B, leaving a layer of the remainder. If the thickness of the layer does not change but the adsorption drops by half, we can deduce that AB lies parallel to the surface and we have again removed either A or B. This is a powerful alternative way of utilizing known defined chemistry in conjunction with a single neutron contrast to explore a layer in much more interesting detail than could be achieved with conventional contrast variation.

Another possibility is to build a theoretical model of the adsorbed layer to evaluate the data (Nylander et al., 2008). Leermakers et al. used self-consistent field modelling to estimate the segment density profiles of adsorbed layers of  $\beta$ -casein on hydrophobic surfaces (Atkinson, Dickinson, Horne, Leermakers, & Richardson, 1996; Leermakers, Atkinson, Dickinson, & Horne, 1996). We have previously found that their modelling of the  $\beta$ -casein layer on the hydrophobic surface is consistent with our neutron reflectometry data (Nylander et al., 2001).

### 3. Results

#### 3.1. Hydrophilic surface

A two-layer optical matrix model was used to fit the neutron reflectivity data obtained from the hydrophilic surface. The data and best fits are shown in Fig. 1 and the fitting parameters for the system in the absence of CPN are shown in Table 1. The fitting parameters used for the system including the CPN are listed in Table 2. Placing the hydrophilic surface in contact with 0.02 M imidazole–HCl buffer (pH 7.0) containing 17 mM  $\text{CaCl}_2$  and 0.1 mg/ml  $\beta$ -casein gave steady state adsorption of  $\beta$ -casein after 2.5 h with a surface excess of 4.0 mg/m<sup>2</sup>. The layer nearest to the surface was 54 Å thick and consisted of 43% protein by volume whereas the outer layer was 42 Å thick but comprised only 15% protein. Rinsing with protein free buffer removed some of the material to give a total adsorbed amount of 2.80 mg/m<sup>2</sup> in inner and outer layers of 40 and 36 Å thickness with protein volume fractions of 43% and 10% respectively. Exposure to 0.04  $\mu\text{g/ml}$  endoproteinase Asp-N in the same buffer solution almost completely removed the protein layer leaving just a thin partial layer of material on the substrate.

The same process was repeated using a 0.1 mg/ml  $\beta$ -casein solution with 17 mM  $\text{CaCl}_2$  in 0.02 M imidazole–HCl buffer (pH 7.0) and, in addition, 13.7 mg/ml CPN. A stable layer was found after 3.5 h of adsorption time and the reflectivity data were again fitted by a two-layer optical matrix model using a partial specific volume of 0.743 ml/g for the combined protein and CPN. These two materials are assumed to have similar scattering length density in D<sub>2</sub>O as discussed in the Materials and methods section and were treated as a single component in the fitting. The fitting parameters are shown in Table 2. It should be noted that the overall thickness and the surface excess are significantly lower than for adsorption in the absence of the CPN. Rinsing the cell had no measurable effect in this instance, suggestive of greater cohesion within the layer. The most striking difference, however, is the failure of the enzyme endoproteinase Asp-N to remove more than 58% of the adsorbed material when nanoclusters were present during the adsorption. This clearly shows that the nanoclusters had reduced the availability of the potential cleavage sites of the protein. The CPN do not adsorb onto the bare silica surface in the absence of  $\beta$ -casein in an otherwise similar solution; both the particles and the surface are negatively charged at pH 7.0.

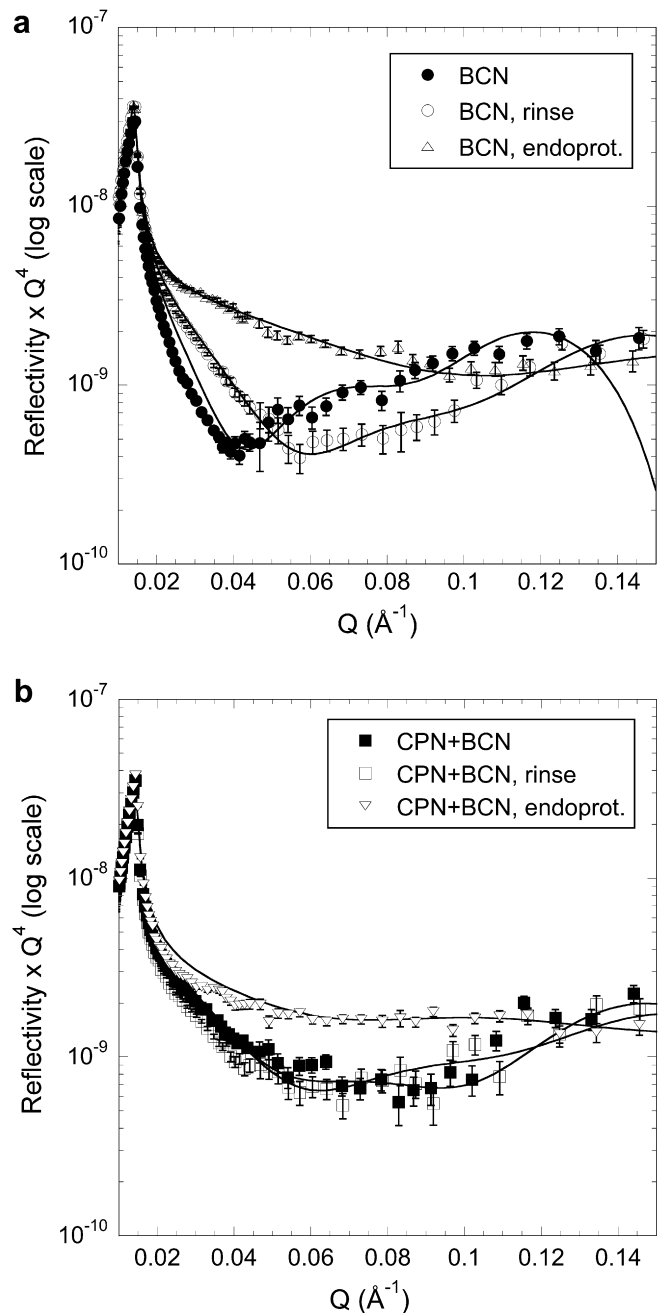


**Fig. 1.** Neutron reflectivity profiles plotted as reflectivity times  $Q^4$  against momentum transfer,  $Q$ , for adsorption at the silica–water interface. The profiles on top (a) show the case of addition of  $\beta$ -casein without particles, those on bottom (b) show the case of simultaneous addition of protein and calcium phosphate nanoclusters followed by addition of enzyme. In (a) BCN refers to the profile obtained after exposure of a clean surface to 0.1 mg/ml  $\beta$ -casein in 0.02 M imidazole–HCl buffer (pH 7.0) containing 17 mM  $\text{CaCl}_2$ . In (b) CPN + BCN refers to the exposure of a second clean surface to a solution of 0.1 mg/ml  $\beta$ -Casein in 0.02 M imidazole–HCl buffer (pH 7.0) containing 17 mM  $\text{CaCl}_2$  and 5 mg/ml calcium phosphopeptide in the form of calcium phosphate nanoclusters. Rinse in each case refers to the profile obtained after rinsing the measuring cell with protein-free and particle-free buffer. Endoprot. refers in each case to the profile obtained from each system after addition of 0.04  $\mu\text{g/ml}$  endoproteinase Asp-N in the buffer subsequent to the rinse.

#### 3.2. Hydrophobic surface

New measurements of  $\beta$ -casein adsorption to the hydrophobic surface in the absence of nanoclusters confirmed earlier work (Fragneto, et al., 1995; T. Nylander et al., 2001). The effects of adding

**Table 1**

The layer thicknesses ( $d_1$ ,  $d_2$ ), scattering length densities ( $\rho_1$ ,  $\rho_2$ ), protein volume fractions ( $\phi_1$ ,  $\phi_2$ ) and surface excesses ( $\Gamma_1$ ,  $\Gamma_2$ ) used to calculate the two-layer fits to the reflectivity data for  $\beta$ -casein adsorbed layer on hydrophilic silica surface. The corresponding reflectivity curves are shown in Fig. 1a. The errors estimation is determined as the limit when the fitted curve falls within the error bars of experimental data. We estimate the error in the scattering density of the protein to  $\pm 0.1 \cdot 10^{-6} \text{ \AA}^{-2}$ , which is due to the uncertainty of the degree of hydrogen/deuterium exchange.

	$\beta$ -Casein <sup>b</sup>	Rinse <sup>c</sup>	Enzyme <sup>d</sup>
$d_1$ (Å)	54 ± 2	40 ± 2	30 ± 3
$d_2$ (Å)	42 ± 3	36 ± 3	0
$\rho_1$ ( $10^6 \text{ \AA}^{-2}$ )	4.8 ± 0.1	4.8 ± 0.1	5.7 ± 0.1
$\rho_2$ ( $10^6 \text{ \AA}^{-2}$ )	5.8 ± 0.1	6.0 ± 0.1	0
$\phi_1$	0.43 ± 0.03	0.43 ± 0.03	0.18 ± 0.03
$\phi_2$	0.15 ± 0.03	0.10 ± 0.03	0
$\Gamma_1$ ( $\text{mg m}^{-2}$ )	3.1 ± 0.2	2.3 ± 0.1	0.7 ± 0.1
$\Gamma_2$ ( $\text{mg m}^{-2}$ )	0.9 ± 0.1	0.5 ± 0.1	0.00
$\Gamma_t$ ( $\text{mg m}^{-2}$ ) <sup>a</sup>	4.0 ± 0.2	2.8 ± 0.1	0.7 ± 0.1

<sup>a</sup>  $\Gamma_t$  is the total surface excess of the two layers combined.

<sup>b</sup>  $\beta$ -Casein refers to the equilibrium state reached in 0.1 mg/ml  $\beta$ -casein solution in 0.02 M imidazole–HCl buffer (pH 7.0) containing 17 mM  $\text{CaCl}_2$ .

<sup>c</sup> Rinse refers to the state after rinsing with protein free buffer.

<sup>d</sup> Enzyme refers to the state after exposure to 0.04  $\mu\text{g/ml}$  endoproteinase Asp-N in the buffer.

the CPN in two different ways were then investigated. In the sequential method, 0.1 mg/ml  $\beta$ -casein was added followed by rinsing with protein-free buffer and then addition of 13.7 mg/ml CPN (sequential addition). In the simultaneous method, the same concentrations of  $\beta$ -casein and CPN were used but in the same solution. All solutions were made up with 0.02 M imidazole–HCl buffer (pH 7.0) containing 17 mM  $\text{CaCl}_2$ . The results shown in Fig. 2 illustrate the difference in neutron reflectivity produced by these two methods.

### 3.2.1. Sequential addition

Sequential addition of  $\beta$ -casein and nanoclusters begins by repeating the earlier experiment on  $\beta$ -casein adsorption onto a hydrophobic surface. At the water/hydrophobized silica interface, the protein layer near the surface reorganizes (Kull et al., 1997; Nylander & Wahlgren, 1994) to expose its more hydrophobic,

**Table 2**

The layer thicknesses ( $d_1$ ,  $d_2$ ), scattering length densities ( $\rho_1$ ,  $\rho_2$ ), protein volume fractions ( $\phi_1$ ,  $\phi_2$ ) and surface excesses ( $\Gamma_1$ ,  $\Gamma_2$ ) used to calculate the two-layer fits to the reflectivity data for  $\beta$ -casein and CPN mixed adsorbed layer onto a hydrophilic silica surface. The corresponding reflectivity curves are shown in Fig. 1b. The errors estimation is determined as the limit when the fitted curve falls within the error bars of experimental data. We estimate the error in the scattering density of the protein to  $\pm 0.1 \cdot 10^{-6} \text{ \AA}^{-2}$ , which is due to the uncertainty of the degree of hydrogen/deuterium exchange.

	$\beta$ -Casein + CPN <sup>b</sup>	Rinse <sup>c</sup>	Enzyme <sup>d</sup>
$d_1$ (Å)	35 ± 2	35 ± 2	35 ± 2
$d_2$ (Å)	33 ± 3	33 ± 3	25 ± 3
$\rho_1$ ( $10^{-6} \text{ \AA}^{-2}$ )	5.1 ± 0.1	5.1 ± 0.1	5.8 ± 0.1
$\rho_2$ ( $10^{-6} \text{ \AA}^{-2}$ )	6.0 ± 0.1	6.0 ± 0.1	6.2 ± 0.1
$\phi_1$	0.35 ± 0.03	0.35 ± 0.03	0.15 ± 0.03
$\phi_2$	0.10 ± 0.03	0.10 ± 0.03	0.04 ± 0.03
$\Gamma_1$ ( $\text{mg m}^{-2}$ )	1.6 ± 0.1	1.6 ± 0.1	0.7 ± 0.1
$\Gamma_2$ ( $\text{mg m}^{-2}$ )	0.4 ± 0.1	0.4 ± 0.1	0.1 ± 0.1
$\Gamma_t$ ( $\text{mg m}^{-2}$ ) <sup>a</sup>	2.1 ± 0.1	2.1 ± 0.1	0.8 ± 0.1

<sup>a</sup>  $\Gamma_t$  is the total surface excess of the two layers combined.

<sup>b</sup>  $\beta$ -Casein + CPN refers to the equilibrium state reached in 0.1 mg/ml  $\beta$ -casein solution in 0.02 M imidazole–HCl buffer (pH 7.0) containing 17 mM  $\text{CaCl}_2$  and 13.7 mg/ml calcium phosphate nanoclusters.

<sup>c</sup> Rinse refers to the state after rinsing with protein and nanocluster free buffer.

<sup>d</sup> Enzyme refers to the state after exposure to 0.04  $\mu\text{g/ml}$  endoproteinase Asp-N in the buffer.

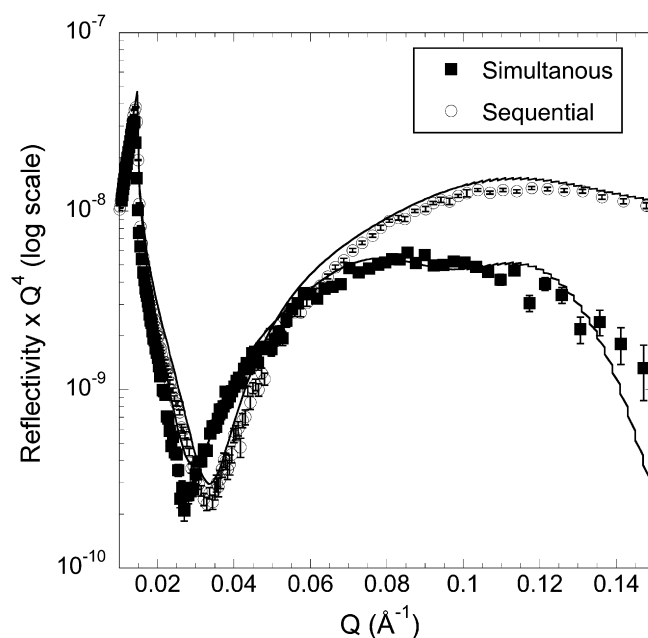


**Fig. 2.** Neutron reflectivity profiles plotted as reflectivity times  $Q^4$  against momentum transfer,  $Q$ , for adsorption at the hydrophobized silica–water interface after adsorption of  $\beta$ -casein and calcium phosphate nanoclusters sequentially and simultaneously. Sequential adsorption was from 0.1 mg/ml  $\beta$ -casein in 0.02 M imidazole–HCl buffer (pH 7.0) containing 17 mM  $\text{CaCl}_2$  followed by rinsing with protein-free buffer and addition of 13.7 mg/ml calcium phosphate nanoclusters in 0.02 M imidazole–HCl buffer (pH 7.0) containing 17 mM  $\text{CaCl}_2$ . Simultaneous adsorption was from 0.1 mg/ml  $\beta$ -casein solution in 0.02 M imidazole–HCl buffer (pH 7.0) containing 17 mM  $\text{CaCl}_2$  and 13.7 mg/ml calcium phosphate nanoclusters.

conformationally flexible (Dalglish & Leaver, 1991) parts to the hydrophobic surface. Hydrophobic groups rich in hydrocarbon moieties have a lower coherent scattering length than hydrophilic groups containing heteroatoms, which are expected to exchange with deuterium in  $\text{D}_2\text{O}$ , due to the negative coherent scattering length of  $^1\text{H}$ . Using the scattering length densities of amino acid residues in  $\text{H}_2\text{O}$  and  $\text{D}_2\text{O}$  and their molecular volumes (Jacrot, 1976), the scattering length density of the most hydrophobic segment of  $\beta$ -casein (residues 94–209) is  $1.54 \cdot 10^{-6} \text{ \AA}^{-2}$  in  $\text{H}_2\text{O}$  and  $2.47 \cdot 10^{-6} \text{ \AA}^{-2}$  in  $\text{D}_2\text{O}$ , whereas the corresponding calculation for the whole protein gives  $1.63 \cdot 10^{-6} \text{ \AA}^{-2}$  in  $\text{H}_2\text{O}$  and  $2.63 \cdot 10^{-6} \text{ \AA}^{-2}$  in  $\text{D}_2\text{O}$ . Thus, this is expected to result in a lower scattering length density very close to the surface than in the rest of the protein layer and so a three-layer fit was used in the optical matrix model for these results. Since the best fit obtained gave a very low scattering length density, about what would be expected of a very dense protein layer (in  $\text{H}_2\text{O}$ ), in the layer close to the surface, we assumed that the solvent content in this inner layer was negligible. The neutron reflectivity data and fits are shown in Fig. 3 and the fitting parameters used are shown in Table 3. Fig. 3a shows the time course of the reflectivity curve after sequential additions with different solutions and Fig. 3b shows the results obtained by the simultaneous method. On exposure to CPN the adsorbed layer became thinner but denser, with an increase in surface excess. The extra material was taken into the outer layer, which contains the phosphate centre that interfaces with the sequestered amorphous calcium phosphate (Holt et al., 1986; Holt et al., 1989; Ono et al., 1994). Exposing the layer to endoproteinase Asp-N solution (0.04  $\mu\text{g/ml}$  in buffer) removed 33% of the adsorbed material – similar to the reduction seen with adsorbed  $\beta$ -casein alone. However, the decrease was much slower when the CPN was present: a stable state being reached after 7 h compared to 3 h in an earlier study using time-resolved ellipsometry (Kull et al., 1997).

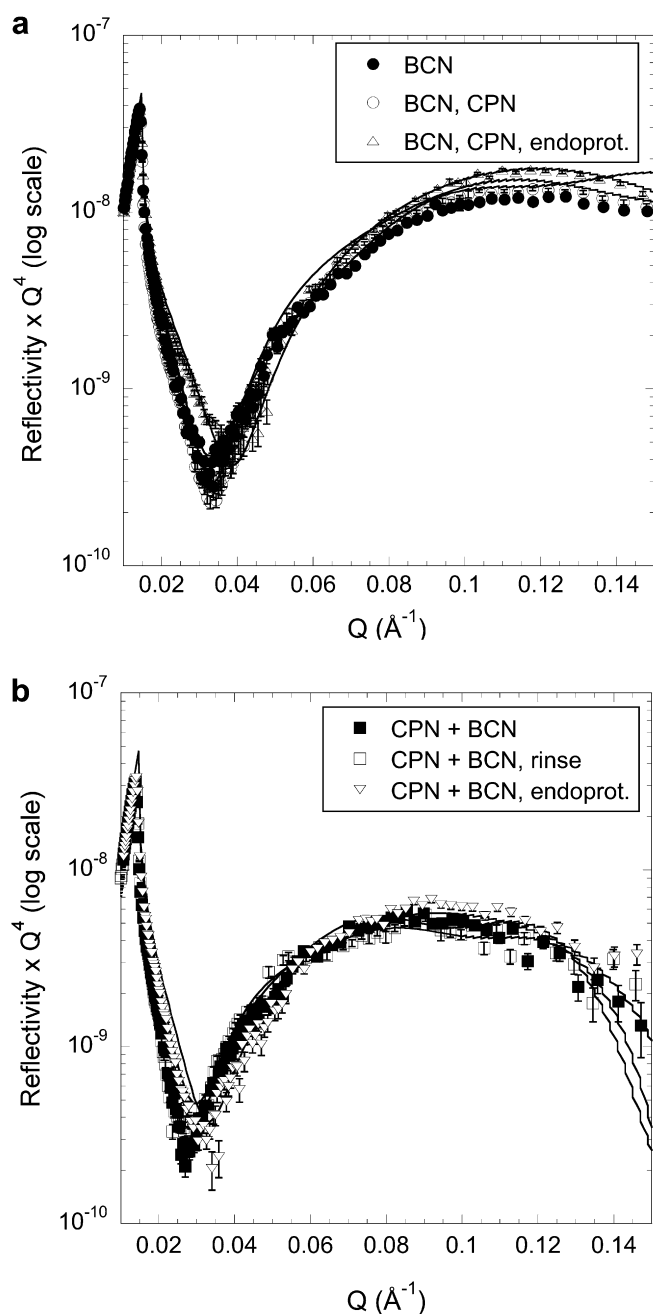


**Fig. 3.** Neutron reflectivity profiles plotted as reflectivity times  $Q^4$  against momentum transfer,  $Q$ , for adsorption at the hydrophobized silica–water interface. The profiles on the left (a) show the results after addition of  $\beta$ -casein followed by sequential addition of calcium phosphate nanoclusters (CPN), those on the right (b) show the case of simultaneous addition of protein and CPN, followed by rinse. BCN refers to the profile obtained after exposure of a clean surface to 0.1 mg/ml  $\beta$ -casein in 0.02 M imidazole–HCl buffer (pH 7.0) containing 17 mM  $\text{CaCl}_2$ . BCN, CPN refers to the same system after rinsing with protein-free buffer and subsequent addition of 13.7 mg/ml calcium phosphate nanoclusters in 0.02 M imidazole–HCl buffer (pH 7.0) containing 17 mM  $\text{CaCl}_2$ . CPN + BCN refers to the profile obtained after exposure of a clean surface to 0.1 mg/ml  $\beta$ -casein solution in 0.02 M imidazole–HCl buffer (pH 7.0) containing 17 mM  $\text{CaCl}_2$  and 13.7 mg/ml calcium phosphate nanoclusters. Rinse refers to the profile obtained after rinsing this second system with protein-free, particle-free buffer. Endoprot. refers in each case to the profile obtained from each system after rinsing with protein-free, nanocluster-free buffer and subsequent addition of 0.04  $\mu\text{g/ml}$  endoproteinase Asp-N in the buffer.

**Table 3**

The layer thicknesses ( $d_1$ ,  $d_2$ ,  $d_3$ ), scattering length densities ( $\rho_1$ ,  $\rho_2$ ,  $\rho_3$ ), protein volume fractions ( $\phi_1$ ,  $\phi_2$ ,  $\phi_3$ ) and surface excesses ( $\Gamma_1$ ,  $\Gamma_2$ ,  $\Gamma_3$ ) used to calculate the three-layer fits to the reflectivity data for  $\beta$ -casein and subsequent CPN adsorption onto a hydrophobized silica surface. The corresponding reflectivity curves are shown in Fig. 3a. The errors estimation is determined as the limit when the fitted curve falls within the error bars of experimental data. We estimate the error in the scattering density of the protein to  $\pm 0.1 \cdot 10^{-6} \text{ \AA}^{-2}$ , which is due to the uncertainty of the degree of hydrogen/deuterium exchange.

	$\beta$ -Casein <sup>b</sup>	CPN <sup>c</sup>	Enzyme <sup>d</sup>
$d_1$ (Å)	14 ± 1	14 ± 1	14 ± 1
$d_2$ (Å)	36 ± 3	30 ± 3	19 ± 3
$d_3$ (Å)	46 ± 5	35 ± 5	32 ± 5
$\rho_1$ ( $10^{-6} \text{ \AA}^{-2}$ )	1.6 ± 0.1	1.6 ± 0.1	1.6 ± 0.1
$\rho_2$ ( $10^{-6} \text{ \AA}^{-2}$ )	5.4 ± 0.1	5.2 ± 0.1	5.5 ± 0.1
$\rho_3$ ( $10^{-6} \text{ \AA}^{-2}$ )	6.0 ± 0.1	6.0 ± 0.1	6.2 ± 0.1
$\phi_1$	1.00 <sup>e</sup>	1.00 <sup>e</sup>	1.00 <sup>e</sup>
$\phi_2$	0.26 ± 0.02	0.32 ± 0.02	0.24 ± 0.02
$\phi_3$	0.10 ± 0.03	0.10 ± 0.03	0.04 ± 0.03
$\Gamma_1$ (mg m <sup>-2</sup> )	1.9 ± 0.1	1.9 ± 0.1	1.9 ± 0.1
$\Gamma_2$ (mg m <sup>-2</sup> )	1.3 ± 0.1	1.3 ± 0.1	0.6 ± 0.1
$\Gamma_3$ (mg m <sup>-2</sup> )	0.6 ± 0.2	0.5 ± 0.2	0.2 ± 0.1
$\Gamma_t$ (mg m <sup>-2</sup> ) <sup>a</sup>	3.8 ± 0.2	3.6 ± 0.2	2.8 ± 0.1

<sup>a</sup>  $\Gamma_t$  is the total surface excess of the three layers combined.

<sup>b</sup>  $\beta$ -Casein refers to the equilibrium state reached in 0.1 mg/ml  $\beta$ -casein solution in 0.02 M imidazole–HCl buffer (pH 7.0).

<sup>c</sup> CPN refers to the equilibrium reached in 17 mM  $\text{CaCl}_2$  and 13.7 mg/ml calcium phosphate nanoclusters in the same buffer.

<sup>d</sup> Enzyme refers to the state after exposure to 0.04  $\mu\text{g/ml}$  endoproteinase Asp-N in the buffer.

<sup>e</sup> Since the best fit obtained gave a very low scattering length density, about what would be expected to a very dense protein layer (in H<sub>2</sub>O), in the layer close to the surface, we assumed that the solvent content in this layer is negligible (see text for further details).

### 3.2.2. Simultaneous addition

Simultaneous addition of  $\beta$ -casein and nanoclusters was investigated using the same solution as for the adsorption onto the hydrophilic surface: 0.1 mg/ml  $\beta$ -casein solution with 17 mM  $\text{CaCl}_2$

**Table 4**

The layer thicknesses ( $d_1$ ,  $d_2$ ,  $d_3$ ), scattering length densities ( $\rho_1$ ,  $\rho_2$ ,  $\rho_3$ ), protein volume fractions ( $\phi_1$ ,  $\phi_2$ ,  $\phi_3$ ) and surface excesses ( $\Gamma_1$ ,  $\Gamma_2$ ,  $\Gamma_3$ ) used to calculate the three-layer fits to the reflectivity data for  $\beta$ -casein + CPN mixture adsorption onto a hydrophobized silica surface. The corresponding reflectivity curves are shown in Fig. 3b. The errors estimation is determined as the limit when the fitted curve falls within the error bars of experimental data. We estimate the error in the scattering density of the protein to  $\pm 0.1 \cdot 10^{-6} \text{ \AA}^{-2}$ , which is due to the uncertainty of the degree of hydrogen/deuterium exchange.

	$\beta$ -Casein + CPN <sup>b</sup>	Rinse <sup>c</sup>	Enzyme <sup>d</sup>
$d_1$ (Å)	37 ± 2	36 ± 2	33 ± 2
$d_2$ (Å)	37 ± 3	37 ± 3	34 ± 3
$d_3$ (Å)	54 ± 5	44 ± 5	34 ± 5
$\rho_1$ ( $10^{-6} \text{ \AA}^{-2}$ )	4.2 ± 0.1	4.4 ± 0.1	4.2 ± 0.1
$\rho_2$ ( $10^{-6} \text{ \AA}^{-2}$ )	5.4 ± 0.1	5.4 ± 0.1	5.6 ± 0.1
$\rho_3$ ( $10^{-6} \text{ \AA}^{-2}$ )	6.1 ± 0.1	6.1 ± 0.1	6.2 ± 0.1
$\phi_1$	0.60 ± 0.03	0.54 ± 0.03	0.60 ± 0.02
$\phi_2$	0.26 ± 0.02	0.26 ± 0.02	0.21 ± 0.02
$\phi_3$	0.07 ± 0.03	0.07 ± 0.03	0.04 ± 0.03
$\Gamma_1$ (mg m <sup>-2</sup> )	3.0 ± 0.2	2.6 ± 0.2	2.7 ± 0.2
$\Gamma_2$ (mg m <sup>-2</sup> )	1.3 ± 0.1	1.3 ± 0.1	1.0 ± 0.1
$\Gamma_3$ (mg m <sup>-2</sup> )	0.5 ± 0.2	0.4 ± 0.2	0.2 ± 0.2
$\Gamma_t$ (mg m <sup>-2</sup> ) <sup>a</sup>	4.8 ± 0.2	4.4 ± 0.2	3.8 ± 0.2

<sup>a</sup>  $\Gamma_t$  is the total surface excess of the three layers combined and the maximum error is estimated to be the same as the maximum error of the layer with largest uncertainty in the surface excess.

<sup>b</sup>  $\beta$ -Casein + CPN refers to the equilibrium state reached in 0.1 mg/ml  $\beta$ -casein solution in 0.02 M imidazole–HCl buffer (pH 7.0) containing 17 mM  $\text{CaCl}_2$  and 13.7 mg/ml calcium phosphate nanoclusters.

<sup>c</sup> Rinse refers to the state after rinsing with protein-free, nanocluster-free buffer.

<sup>d</sup> Enzyme refers to the state after exposure to 0.04  $\mu\text{g/ml}$  endoproteinase Asp-N in the buffer.

in 0.02 M imidazole–HCl buffer (pH 7.0) and at a CPN concentration of 13.7 mg/ml and the results are presented in Fig. 3b. A three-layer model was used again and the fitting parameters are shown in Table 4. It should be noted that a much thicker layer resulted with a higher surface excess and a more even density profile, and that the enzyme only removed 13% of the adsorbed material.

### 3.3. Following the kinetics

To record a neutron reflection profile over the full range of momentum transfer with good statistics took around 3 h but a measurement at one angle and low momentum transfer could be taken in 20 min. The time to reach a stable state after adsorption or desorption in these experiments was up to 7 h in some cases, allowing the kinetics to be followed. A system was considered to have reached a steady state when no further change was seen in its reflectivity profile after a further hour of equilibration. Two good examples are shown in Fig. 4. Here it should be noted that the kinetic data was obtained only at the lower angle. The fits to the kinetic data are based on the fit to the reflectometry curve recorded over the full Q-range (parameters in Table 2 for  $\beta$ -casein and CPN adsorption and Table 3). The first example, Fig. 4a, shows the progress of the adsorption of protein and CPN together onto a hydrophilic silica surface from a solution containing 0.1 mg/ml

$\beta$ -casein and 17 mM  $\text{CaCl}_2$  in 0.02 M imidazole–HCl buffer (pH 7.0) with CPN at a concentration of 13.7 mg/ml in  $\text{D}_2\text{O}$ . The data and best fits are shown for the runs recorded 0.5, 1.5, 2.5 and 3.5 h after addition of the solution to the sample cell. To highlight the differences from one fit to the next, the four fits are shown superimposed on a separate graph (Fig. 4c). It turns out that the kinetics of the adsorption can be modelled as an increase in the thickness,  $d_1$ , of the inner layer in the sequence 20, 25, 30 and 35 Å after 0.5, 1.5, 2.5 and 3.5 h, respectively. A corresponding change in the thickness of the outer layer (with very low protein/CPN density) would not have sufficient effect on the reflectivity at the lower angle used to record the kinetic data to be significant at the short counting time used, due to very low protein/CPN density in that layer. A second example is provided by the action of the enzyme endoproteinase Asp-N on the adsorbed layer after sequential addition of  $\beta$ -casein and CPN to a hydrophobic surface. The data are presented in Fig. 4b and d. The major effect of the endoproteinase Asp-N was found to be a decrease in thickness of the outer layers. Good fit could be obtained using  $d_2$  values of 30, 27 and 19 Å after 2, 4 and 7 h, respectively. The density of matter in the outermost layer is very low and due to the short counting time and the measurement at only one angle, the changes in the outermost layers with time could not be determined. These data confirm the suggested orientation of  $\beta$ -casein on the surface and hence validate the model used.

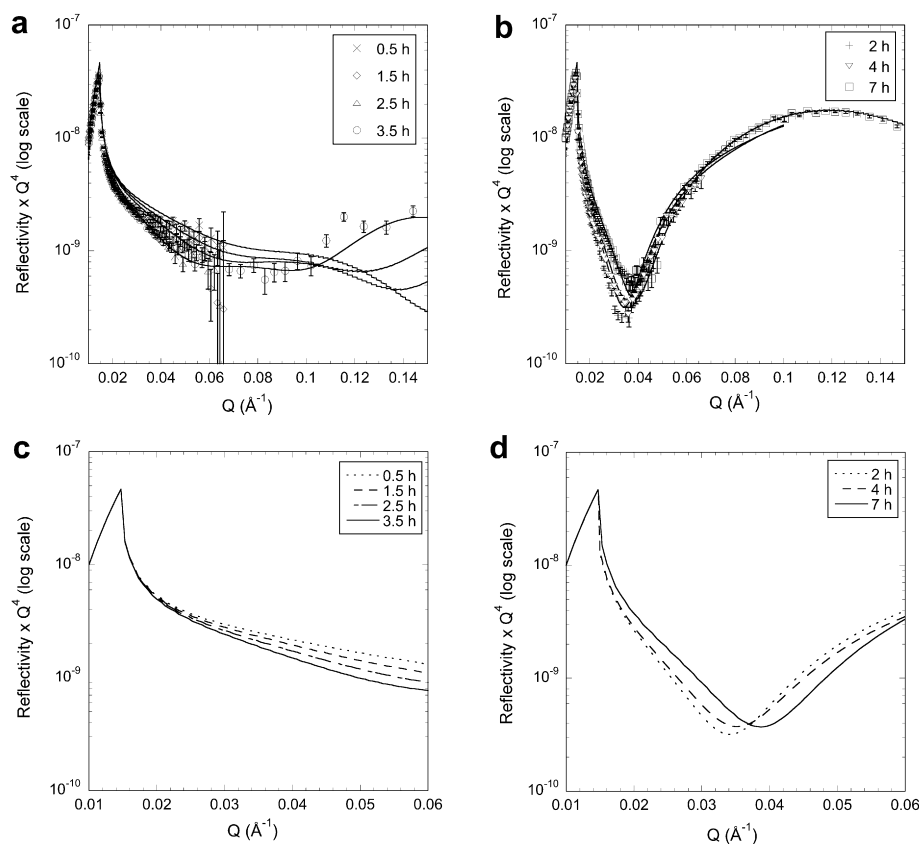


**Fig. 4.** Following kinetics of adsorption using neutron reflection with Neutron reflectivity profiles plotted as reflectivity times  $Q^4$  against momentum transfer,  $Q$  for different equilibration times. The two examples shown are of simultaneous addition of  $\beta$ -casein and nanoclusters to a hydrophilic surface in Fig. a, c and of the action of the enzyme Endoproteinase Asp-N on the adsorbed layer after sequential addition of  $\beta$ -casein and nanoclusters to a hydrophobic surface in Fig. b, d. The protein was adsorbed from 0.1 mg/ml  $\beta$ -casein and 17 mM  $\text{CaCl}_2$  in 0.02 M imidazole–HCl buffer (pH 7.0) in  $\text{D}_2\text{O}$ , the cell was rinsed with protein-free, particle-free buffer, nanoclusters were adsorbed from 17 mM  $\text{CaCl}_2$  in 0.02 M imidazole–HCl buffer (pH 7.0) using calcium phosphate nanoclusters concentration of 13.7 mg/ml before another rinse and addition of endoproteinase Asp-N solution (0.04  $\mu\text{g/ml}$  in buffer). The fits to the kinetic data are based on the fit to the reflectometry curve recorded over the full Q-range (parameters in Table 2 for  $\beta$ -casein and CPN adsorption and Table 3). Mixed  $\beta$ -casein and CPN adsorption was modeled as an increase in the thickness,  $d_1$ , of the inner layer in the sequence 20 Å, 25 Å, 30 Å and 35 Å after 0.5, 1.5, 2.5 and 3.5 h, respectively. For the kinetics of the endoproteinase Asp-N action, the model used to fit the data was the same as given in Table 3 with a decrease in  $d_2$  from 30, 27, 19 Å after 2, 4 and 7 h, respectively. For the sake of clarity the theoretical fitted profiles based on the data in Fig. 4a and b, respectively, for simultaneous addition of  $\beta$ -casein and nanoclusters to a hydrophilic surface are shown in Fig. 4c and for the action of the enzyme Endoproteinase Asp-N on the adsorbed layer after sequential addition of  $\beta$ -casein and nanoclusters to a hydrophobic surface in Fig. 4d.

#### 4. Discussion

The CPN are thermodynamically stable particles with an equilibrium size determined by a balance between a positive free energy change in the formation of the calcium phosphate core and a negative free energy change in the sequestration of the core by a shell of phosphopeptides (Holt et al., 2009). They can be formed by a “forward” reaction in which calcium phosphate precipitates from solution in the presence of the phosphopeptide or from a “back” reaction in which a preformed precipitate of amorphous calcium phosphate is sequestered by the addition of the phosphopeptide (Little & Holt, 2004). Although the exchange of calcium and phosphate ions between the nanocluster and solution is relatively fast, the exchange rate of the peptide is slow on the NMR timescale (Holt et al., 1996). Nevertheless, exchange of the peptide occurs over hours or longer. Thus in principle, one or more phosphopeptides could exchange with the same number of whole  $\beta$ -casein molecules to allow the modified nanoclusters to accumulate by adsorption at the silica interface. It might also be reasonable to assume that for a natively unfolded protein, the affinity is determined by the sequence of phosphorylated residues and is largely independent of the length of the phosphopeptide and so, mole by mole, the whole protein is about as effective at sequestering the calcium phosphate as is the shorter peptide. Under our experimental conditions, significant adsorption of the modified nanoclusters would therefore be expected.

##### 4.1. Hydrophilic surface

The results of the experiments on the hydrophilic silica surface show that calcium phosphate nanoclusters in the  $\beta$ -casein solution were adsorbed with the protein at the solid–liquid interface. The presence of the CPN reduced both the rate and degree of adsorption of protein onto the silica as determined by neutron reflection. The volume fraction profiles in the direction normal to the surface are shown in Fig. 5, the total volume fraction of protein and particles is plotted. The effect on the degree of adsorption implies that some calcium phosphate was adsorbed along with the  $\beta$ -casein at the surface and the effect on the rate implies that a degree of binding between protein and particles occurred in the bulk solution. This may have affected the affinity of the  $\beta$ -casein for the hydrophilic silica surface either through direct binding to the phosphorylated part of the protein or through allosteric effects resulting from that binding, or both. The adsorbed material was more firmly secured to the surface than in the absence of the CPN; rinsing with protein free buffer had no effect on the mixed layer whereas without the inclusion of nanoclusters half the layer was removed. After rinsing, treatment of the  $\beta$ -casein adsorbate lacking CPN with the proteolytic enzyme Endoproteinase Asp-N removed 73% of the material but when CPN was present only around 57% of the layer was removed. This suggests that the two protein cleavage sites near the binding sites for the calcium phosphate were less available to the enzyme in the latter case; these sites are known to be in the highly phosphorylated hydrophilic N-terminal section of the protein (Wahlgren, Dejmeek, & Drakenberg, 1994). It is highly likely that it is the binding of the  $\beta$ -casein to the CPN near these sites that renders them inaccessible to the proteolytic enzyme.

##### 4.2. Hydrophobic surface

The timing of the introduction of calcium phosphate to the system was investigated in the experiments on the hydrophobic surface. In one case the  $\beta$ -casein solution was added first, and the CPN were added afterwards. The volume fraction profiles for this system is shown in Fig. 6. The first part of this experiment is

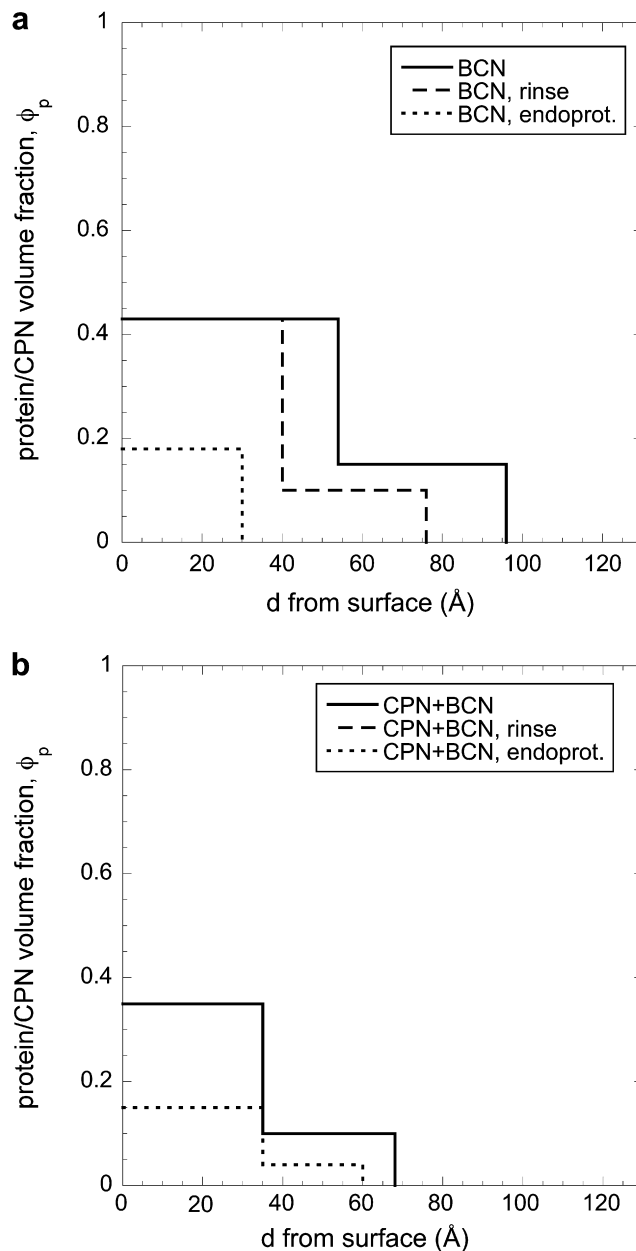


**Fig. 5.** Volume fraction of  $\beta$ -casein and calcium phosphate nanoclusters (CPN) summed as a function of distance from the silica surface, where a.) shows the system in the absence of calcium phosphate and b.) shows the system including calcium phosphate nanoclusters. The solid line shows the profile after addition of  $\beta$ -casein (with CPN in the lower graph), the dashed line shows the profile after rinsing with protein-free, particle-free buffer. In b.) this is exactly overlaid on the solid black line. The dotted line shows the profile after treatment with endoproteinase Asp-N.

a reproduction of earlier work in which the adsorption of  $\beta$ -casein at a hydrophobized silica surface in the presence of calcium ions was studied (Nylander et al., 2001) and is used as a comparison for the system in the presence of the CPN. Subsequent addition of the CPN slightly reduced the amount of adsorbed material and the overall layer thickness but also decreased the fraction of water in the layer. The process was complete in five hours, a timescale that allowed the kinetics to be studied conveniently by neutron reflection. That the nanoclusters are incorporated into the surface layer was shown by the effect of the proteolytic enzyme Endoproteinase Asp-N. In the absence of CPN, the enzyme removed over half of the adsorbed  $\beta$ -casein layer in only half an hour. When CPN was added to the

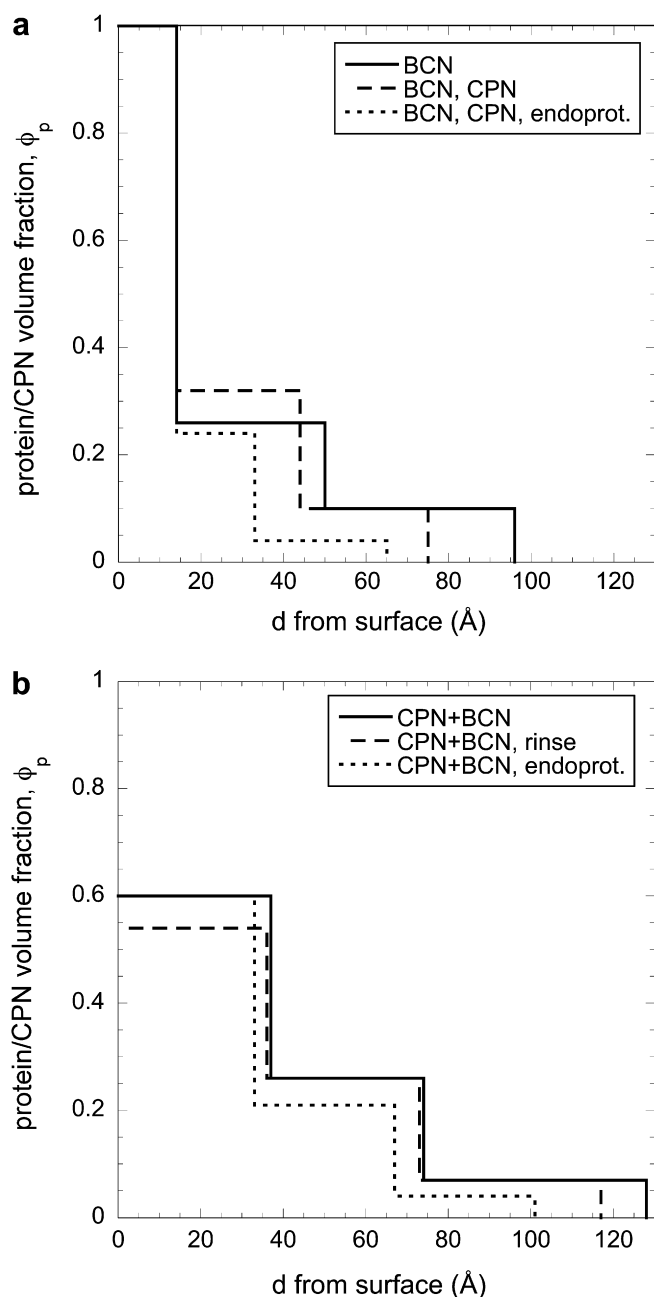


**Fig. 6.** Volume fraction of  $\beta$ -casein and calcium phosphate nanoclusters (CPN) summed as a function of distance from the hydrophobized silica surface, where a.) shows the density profile when  $\beta$ -casein was added before exposure to nanoclusters and b.) shows the density profile when  $\beta$ -casein and CPN were added together in the same solution. The solid line shows the profile after the first addition step, the dashed line in a.) shows the profile after exposure to nanoclusters and b.) shows the profile after rinsing with protein-free, particle-free buffer. The dotted line in each graph shows the profile after exposure to endoproteinase Asp-N.

protein layer only a quarter of the adsorbed material was removed in seven hours. This implies that the two potential protein cleavage sites available to Endoproteinase Asp-N that were open to attack in the earlier work on the protein-only system are at least partially blocked by conformational changes or steric hindrance in the presence of the CPN. These sites are located in the hydrophilic N-terminal region of  $\beta$ -casein, which is known to bind selectively calcium.

When  $\beta$ -casein solution containing CPN was placed in contact with the hydrophobized surface, much more material was

adsorbed. The time taken to reach equilibrium was 2.5 h, as for the case of  $\beta$ -casein adsorption onto a hydrophobic surface in the absence of CPN, but an additional 27% was adsorbed with CPN added simultaneously compared with the protein alone. The increase in adsorbed amount was 24% compared to the sequential adsorption of  $\beta$ -casein and CPN. Thus the results suggest the total amount adsorbed slightly decreased when CPN was sequentially added to the layer although the amount in layer 2 increased slightly (Table 3). Rinsing with buffer only removed a small fraction ( $\approx 9\%$ ) of the material adsorbed when  $\beta$ -casein and CPN were added simultaneously and treatment of the remainder with the proteolytic enzyme Endoproteinase Asp-N only removed a further 13% of the layer compared with around a quarter in the case of protein adsorption followed by addition of the CPN (Table 3) or about 30% in the complete absence of the CPN (Nylander et al., 2001). This process was complete in less than two hours, which suggests that only the outermost protein parts of the layer were available for attack by the enzyme. This is confirmed by the changes in density profiles as given in Fig. 6. In this case, the calculations show that even more of the hydrophilic part of the protein must be bound to the CPN than when the nanoclusters are added subsequent to  $\beta$ -casein adsorption on the hydrophobic surface. This is not surprising, given that adsorption of the amphiphilic protein to the hydrophobic surface in water necessarily involves the attachment of the hydrophobic section of the protein to the solid surface and the exposure of the hydrophilic and the calcium binding part of  $\beta$ -casein to the bulk water. This fixing of the orientation of the hydrophilic part of the  $\beta$ -casein molecules towards the aqueous phase will make them readily available to bind CPN from the bulk solution.

## 5. Conclusions

Calcium phosphate nanoclusters had a strong effect on the adsorption of  $\beta$ -casein onto hydrophilic and hydrophobic surfaces. The degree and the kinetics of adsorption were affected, as was the conformation of the protein. The time at which the nanoclusters were introduced had a large effect on  $\beta$ -casein adsorption on the hydrophobic surface. Neutron reflection was used successfully to follow the kinetics of the adsorption and desorption processes and to give conformational information on the protein via the use of a selective proteolytic enzyme.

Whereas  $\beta$ -casein adsorbed to both the hydrophilic and the hydrophobic silica surfaces, the CPN formed by the N-terminal tryptic phosphopeptide of  $\beta$ -casein adsorbed to neither. Notwithstanding this, mixtures of the two formed a surface layer whose structure was markedly different to that of the  $\beta$ -casein alone. A reasonable explanation is that  $\beta$ -casein and the  $\beta$ -casein phosphopeptide can exchange in the shell of the nanocluster to make it surface active.

## Acknowledgements

Hanna Wacklin is acknowledged for constructive and inspiring discussion as well as generous help during the experiment. The Swedish Research Council is thanked for financial support and the Institut Laue-Langevin, France, is thanked for allocations of neutron beam time.

## References

- Atkinson, P. J., Dickinson, E., Horne, D. S., Leermakers, F. A. M., & Richardson, R. M. (1996). Theoretical and experimental investigations of adsorbed protein structure at a fluid interface. *Berichte der Bunsengesellschaft für physikalische Chemie*, 100, 994–998.

- Atkinson, P. J., Dickinson, E., Horne, D. S., & Richardson, R. M. (1995). Neutron reflectivity of adsorbed  $\beta$ -casein and  $\beta$ -lactoglobulin at the air-water interface. *Journal of the Chemical Society, Faraday Transactions*, 91, 2847–2854.
- Born, M., & Wolf, E. (1980). *Principles of optics* (6th ed.). Cambridge: Cambridge University Press.
- Brooksbank, D. V., Davidson, C. M., Horne, D. S., & Leaver, J. (1993). Influence of electrostatic interactions on b-casein layers adsorbed on polystyrene latices. *Journal of the Chemical Society, Faraday Transactions*, 89, 3419–3425.
- Clegg, R. A., & Holt, C. (2009). An E. coli over-expression system for multiply-phosphorylated proteins and its use in a study of calcium phosphate sequestration by novel recombinant phosphopeptides. *Protein Expression and Purification*, 67, 23–34.
- Cubitt, R., & Fragneto, G. (2002). D17: the new reflectometer at the ILL. *Applied Physics A—Material Science and Processing*, 74, S329–S331.
- Dagleish, D. G., & Leaver, J. (1991). The possible conformations of milk proteins adsorbed on oil/water interfaces. *Journal of Colloid and Interface Science*, 141, 288–294.
- Dickinson, E. (1999). Adsorbed protein layers at fluid interfaces: interactions, structure and surface rheology. *Colloids Surfaces B: Biointerfaces*, 15, 161–176.
- Dickinson, E., Horne, D. S., Phipps, J. S., & Richardson, R. M. (1993). A neutron reflectivity study of the adsorption of  $\beta$ -casein at fluid interfaces. *Langmuir*, 9, 242–248.
- Drapeau, G. R. (1980). Substrate specificity of a proteolytic enzyme isolated from a mutant of *Pseudomonas fragi*. *The Journal of Biological Chemistry*, 255, 839–840.
- Efimova, Y. M., van Well, A. A., Hanefeld, U., Wierczynski, B., & Bouwman, W. G. (2005). On the scattering length density of proteins in  $H_2O/D_2O$ : determination of H–D exchange using  $ES^{+1}$ -MS. *Journal of Radioanalytical and Nuclear Chemistry*, 264, 271–275.
- Fragneto, G., Lu, J. R., McDermott, D. C., & Thomas, R. K. (1996). Structure of monolayers of tetraethylene glycol monododecyl ether Adsorbed on self-assembled monolayers on silicon: a neutron reflectivity study. *Langmuir*, 12, 477–486.
- Fragneto, G., Thomas, R. K., Rennie, A. R., & Penfold, J. (1995). Neutron reflection study of bovine beta-casein adsorbed on OTS self-assembled monolayers. *Science*, 267, 657–660.
- Holt, C. (1998). Casein micelle substructure and calcium phosphate interactions studied by saphacryl column chromatography. *Journal of Dairy Science*, 81, 2994–3003.
- Holt, C., Davies, D. T., & Law, A. J. R. (1986). Effects of colloidal calcium-phosphate content and free calcium-ion concentration in the milk serum on the dissociation of bovine casein micelles. *Journal of Dairy Research*, 53, 557–572.
- Holt, C., & Sawyer, L. (1988). Primary and predicted secondary structure of the caseins in relation to their biological role. *Protein Engineering*, 2, 251–259.
- Holt, C., Sørensen, E. S., & Clegg, R. A. (2009). Role of calcium phosphate nanoclusters in the control of calcification. *FEBS Journal*, 276, 2308–2323.
- Holt, C., Timmins, P. A., Errington, N., & Leaver, J. (1998). A core-shell model of calcium phosphate nanoclusters stabilised by b-casein phosphopeptides, derived from sedimentation equilibrium and small-angle X-ray and neutron-scattering measurements. *European Journal of Biochemistry*, 252, 73–78.
- Holt, C., van Kemenade, M. J. J. M., Nelson, L. S., Sawyer, L., Harries, J. E., Bailey, R. T., et al. (1989). Composition and structure of micellar calcium-phosphate. *Journal of Dairy Research*, 56, 411–416.
- Holt, C., Wahlgren, N. M., & Drakenberg, T. (1996). Ability of a  $\beta$ -casein phosphopeptide to modulate the precipitation of calcium phosphate by forming amorphous dicalcium phosphate nanoclusters. *Biochemical Journal*, 314, 1035–1039.
- Jacrot, B. (1976). The study of biological structures by neutron scattering from solution. *Reports on Progress in Physics*, 39, 911–953.
- Kull, T., Nylander, T., Tiberg, F., & Wahlgren, N. M. (1997). Effect of surface properties and added electrolyte on the structure of  $\beta$ -casein layers adsorbed at the solid/aqueous interface. *Langmuir*, 13, 5141–5147.
- Leaver, J., & Dagleish, D. G. (1992). Variations in the binding of  $\beta$ -casein to oil-water interfaces detected by trypsin-catalysed hydrolysis. *Journal of Colloid and Interface Science*, 149, 49–55.
- Leclerc, E., & Calmettes, P. (1997). Interactions in micellar solution of  $\beta$ -casein. *Physical Review Letters*, 78, 150–153.
- Leermakers, F. A. M., Atkinson, P. J., Dickinson, E., & Horne, D. S. (1996). Self-consistent-field modeling of adsorbed beta-casein: effects of pH and ionic strength on surface coverage and density profile. *Journal of Colloid and Interface Science*, 178, 681–693.
- Little, E. M., & Holt, C. (2004). An equilibrium thermodynamic model of the sequestration of calcium phosphate by casein phosphopeptides. *European Biophysics Journal*, 33, 435–447.
- Lu, J. R., & Thomas, R. K. (2000). The application of neutron and X-ray specular reflection to proteins at interfaces. In A. Baszkin, & W. Norde (Eds.), *Physical chemistry of biological interfaces* (pp. 609–650). New York: Marcel Dekker.
- Mackie, A. R., Mingins, J., & North, A. N. (1991). Characterisation of adsorbed layers of a disordered coil protein on polystyrene latex. *Journal of Chemical Society, Faraday Transactions*, 87, 3043–3049.
- Nylander, T., Campbell, R. A., Vandoolaeghe, P., Cardenas, M., Linse, P., & Rennie, A. R. (2008). Neutron reflectometry to investigate the delivery of lipids and DNA to interfaces (Review). *Biointerphases*, 3, FB64–FB82.
- Nylander, T., & Tiberg, F. (1999). Wetting of  $\beta$ -casein layers adsorbed at the solid/aqueous interface. *Colloids Surfaces B: Biointerfaces*, 15, 253–261.
- Nylander, T., Tiberg, F., Su, T.-J., Lu, J. R., & Thomas, R. K. (2001).  $\beta$ -casein adsorption at the hydrophobised silicon oxide – aqueous solution interface and the effect of added electrolyte. *Biomacromolecules*, 2, 278–287.
- Nylander, T., & Wahlgren, N. M. (1994). Competitive and sequential adsorption of  $\beta$ -casein and  $\beta$ -lactoglobulin on hydrophobic surfaces and the interfacial structure of  $\beta$ -casein. *Journal of Colloid and Interface Science*, 162, 151–162.
- Nylander, T., & Wahlgren, N. M. (1997). Forces between adsorbed layers of  $\beta$ -casein. *Langmuir*, 13, 6219–6225.
- Ono, T., Ohotawa, T., & Takagi, Y. (1994). Complexes of casein phosphopeptide and calcium-phosphate prepared from casein micelles by tryptic digestion. *Bioscience Biotechnology and Biochemistry*, 58, 1376–1380.
- Payens, T. A. J., & Vreeman, H. J. (1982). Casein micelles and micelles of  $\kappa$ - and  $\beta$ -casein. In K. L. Mittal (Ed.), *Solution behaviour of surfactants, Vol. 1* (pp. 543–571). New York: Plenum.
- Penfold, J., Richardson, R. M., Zarbakhsh, A., Webster, J. R. P., Bucknall, D. G., Rennie, A. R., et al. (1997). Recent advances in the study of chemical surfaces and interfaces by specular neutron reflection. *Journal of Chemical Society, Faraday Transactions*, 93, 3899–3917.
- Wahlgren, N. M. (1992). *A nuclear magnetic resonance approach to the milk system*. PhD thesis, University of Lund, Sweden.
- Wahlgren, N. M., Dejmeck, P., & Drakenberg, T. (1994). Secondary structures in  $\beta$ -casein peptide 1–42: a two dimensional nuclear magnetic resonance study. *Journal of Dairy Research*, 61, 495–506.
- Walstra, P., & Jenness, R. (1984). *Dairy chemistry and physics*. New York: Wiley-Interscience.